Image-based modelling using geometric surface partial differential equations (GS-PDEs)

Anotida Madzvamuse
In collaboration with FengWei Yang, Chadrasekhar Venkataraman and Vanessa Styles

University of British Columbia

European Union

am823@math.ubc.ca

JMM2023, 12th April 2023, Institute of Mathematics, Lodz University of Technology

Data-driven coupled bulk-surface and ECM models for cell motility and pattern formation

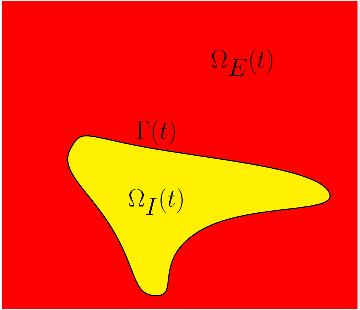

Aim: To develop a mathematical and computational framework for modelling cell motility and pattern formation

1. Data-driven Modelling and Analysis:
    - **Mechanics**: Viscoelastic, poroelastic, hyperelastic, morphoelastic in the cell interior and ECM, Geometric Surface PDEs on the cell surface: *Protrusion, Retraction, Adhesion, Membrane forces such as surface tension and bending rigidity*, . . .
    - **Biochemistry**: Polarisation, Receptor-Ligand Dynamics, Spatio-temporal dynamics of RhoGTPases, . . .
2. Numerical Analysis and HPC Scientific Computing: Development of accurate, robust and efficient numerical methods for simulating the model equations
3. Validation and Model Predictions: Calibrate and test model predictions with experimental data
4. Parameter Identification and Model Selection: Bayesian and optimal control approaches (useful for guiding data acquisition)

Whole cell tracking through an optimal control of geometric evolution laws

- Yang, F., Venkataraman, C., Gu, S., Styles, V. and Madzvamuse, A., 2022. *Force estimation during cell migration using mathematical modelling*. Journal of Imaging, **8**(7), p.199. doi.org/10.3390/jimaging8070199
- Yang, F.W. Venkataraman, C. Styles, V. and Madzvamuse, A. (2017). *A robust and efficient adaptive multi-grid solver for the optimal control of phase field formulations of geometric evolution laws.* Communications in Computational Physics. **21**(1):65-92. doi: 10.4208/cicp.240715.080716a
- Yang, F.W. Venkataraman, C. Styles, V. Kuttenberger, V. Horn, E. von Guttenberg, Z. and Madzvamuse, A. (2016). *A computational framework for particle and whole cell tracking applied to a real biological dataset*. Journal of Biomechanics. ISSN 0021-9290
- Blazakis, K.N. Madzvamuse, A. Reyes-Aldasoro, C.C. Styles, V. and Venkataraman, C. (2015) *Whole cell tracking through the optimal control of geometric evolution laws* Journal of Computational Physics, **297**. pp. 495-514. ISSN 0021-9991
- Yang, F.W. Venkataraman, C, Styles, V and Madzvamuse, A. (2015) *A parallel and adaptive multi-grid solver for the solutions of the optimal control of geometric evolution laws in two and three dimensions*. In: 4th International Conference on Computational and Mathematical Biomedical Engineering - CMBE2015. P. Nithiarasu and E. Budyn (Eds.) 29 June-1 July 2015, Paris, France.
- Blazakis, K.N. Reyes-Aldasoro, C C, Styles, V, Venkataraman, C and Madzvamuse, A. (2015) *An optimal control approach to cell tracking*. In: Louis, Alfred K, Arridge, Simon and Rundell, Bill (eds.) Proceedings of the Inverse Problems from Theory to Applications Conference (IPTA2014). IOP Publishing Ltd , pp. 74-77. ISBN 9780750311069

Biological Motivation: Zebrafish as model organism

- Zebrafish are transparent - observe morphological changes during development.
- Use the GFP to label individual cells, organs or even organelles.
- Embryo development in normal/abnormal situations (mutated or drugs)
- Zebrafish are more closely related to humans than invertebrate models such as the worm *C. elegans* and the fly *D. Melanogaster*,

Zebrafish larva three days post-fertilisation

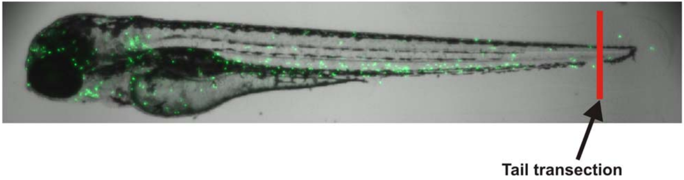

Neutrophil cell migration during wound healing process

Cell migration during wound healing process

3-D reconstruction of the cell migration

Discrete sequence of cross-sections of 3D image datasets

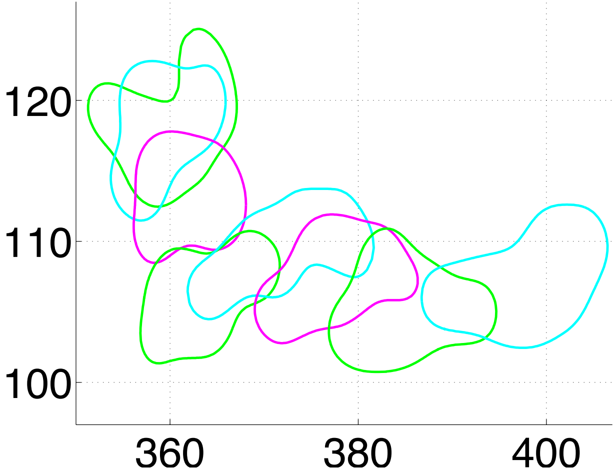

- Can we model "optimally" the evolution of the cell from one image to the next?
- Reconstruct dynamic evolution of the cell from static images?

Cell Tracking

- Reconstruct a dynamic (2D+t) or (3D+t) model from static imaging data (2D or 3D).
    - Particle tracking (e.g. Agent Based Tracking): recover trajectories, “connect the dots”, enables the computation of many motility related statistics such as velocities, persistence lengths, MSD, etc.
    - Whole cell tracking: recover morphologies, allows investigation of the dynamics of geometric features (surface area, volume, curvature, aspect ratio, . . .)
- For example
    - **Particle tracking**: reconstruct (often only centroid) trajectories by linear interpolation
    - **Whole Cell tracking**: Level set and electrostatic based methods that generate trajectories for marker points on the membrane

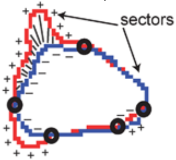

[Tyson, Epstein, Anderson, and Bretschneider, 2010]

- Our approach: fitting a mathematical model to static imaging data.

Whole Cell Tracking

Basic Idea: Reconstruct (dynamic) whole cell morphologies from static imaging data.

- Majority of existing approaches (level set, electrostatics, ...) incorporate only geometric considerations equidistribution of vertices, ...
- Our approach: Fit models for the cell evolution to imaging data. Focus is on geometric evolution law based models for the motion of the cell membrane as considered in [Barreira, Elliott, and Madzvamuse, 2011; Elliott, Stinner, and Venkataraman, 2012; Marth and Voigt, 2013; Neilson, Veltman, van Haastert, Webb, Mackenzie, and Insall, 2011; Shao, Levine, and Rappel, 2012].
- For many cell tracking scenarios, only the membrane location is available with no other fluorescence data provided, hence we focus on this most basic setting.

Geometric Evolution Law Model

$$\begin{aligned} \boldsymbol{V}(\vec{x},t)\boldsymbol{n}(\vec{x},t) &= (\eta(\vec{x},t) \quad + \lambda(t) \quad - \sigma H(\vec{x},t))\boldsymbol{n}(\vec{x},t) \qquad (\vec{x},t) \in (\Gamma(t),[0,T]) \\ \text{Velocity} \quad &= \text{Forcing} + \text{Vol. Cons.} + \text{Regularisation} \end{aligned}$$

The problem is to find $\eta(\vec{x},t)$ such that the solution to the model and the image data are “close”.

Problem is in effect the optimal control of the sharp interface formulation of a geometric evolution law for which no adequate theory is available yet (how to define a smooth notion of “closeness”, regularity for $\eta(\vec{x},t)$, etc).

Diffuse Interface Formulation

From Sharp to Diffuse Interface

Given a surface

$$\Gamma = \{\vec{x} \in \Omega | d_\Gamma(x) = 0\},$$

where d_Γ is the signed distance function to Γ, compute $\varphi : \Omega \to \mathbb{R}$ such that

$$\varphi_\epsilon(\vec{x}) = \begin{cases} 1 & \text{if } d_\Gamma(\vec{x}) > \epsilon \\ \sin\left(\frac{\pi d_\Gamma(\vec{x})}{2\epsilon}\right) & \text{if } \left|d_\Gamma(\vec{x})\right| < \epsilon \\ -1 & \text{if } d_\Gamma(\vec{x}) < -\epsilon \end{cases}$$

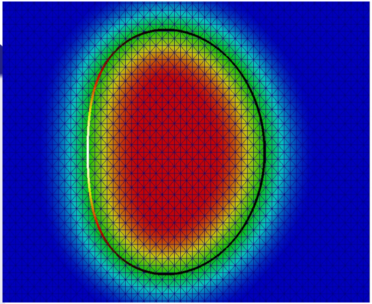

Alternatively one may simply work with (high contrast) raw data without further segmentation of the cell outline (with a few steps of de-noising).

Individual cells

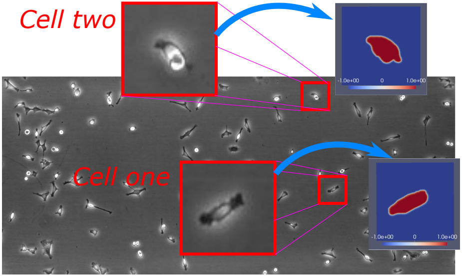

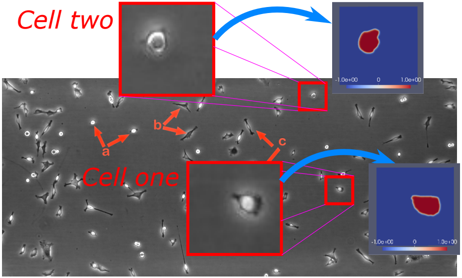

Diffuse Interface Formulation

Adopting a phase field (diffuse interface) formulation $\rightsquigarrow$ Allen-Cahn with forcing.

Allen-Cahn with forcing

$$\varepsilon \partial_t \varphi(\mathbf{x}, t) = \varepsilon \Delta \varphi(\mathbf{x}, t) - \frac{1}{\varepsilon} G'(\varphi(\mathbf{x}, t)) + c_w \eta(\mathbf{x}, t) + \lambda(t) \quad \vec(x, t) \in \Omega \times [0, T] \tag{1}$$

where $G(\varphi) = \frac{1}{4}(\varphi^2 - 1)^2$ is a double well potential with minima at ± 1.
Volume constraint interpreted as constraint on the mass, i.e., $\int_\Omega \varphi$.
Example: fitting to a single image φ_{des} (using an observation at a previous time as initial data).

PDE constrained optimisation problem

$$\min J(\varphi, \eta) = \frac{1}{2} \int_\Omega \left(\varphi(\mathbf{x}, T) - \varphi_{des}(\mathbf{x})\right)^2 d\mathbf{x} + \frac{\gamma}{2} \int_0^T \int_\Omega \eta^2 d\mathbf{x} dt$$

subject to (1).

Following [Haußer, Rasche, and Voigt, 2010; Haußer, Janssen, and Voigt, 2012] we formally derive the first order optimality conditions and propose an adjoint based solution method for the minimisation problem.

Optimality conditions [Tröltzsch, 2010]

Introducing the Lagrange multiplier (adjoint state) p, we define the Lagrangian functional

$$\mathcal{L}(\varphi,\eta,p) = J(\varphi,\eta) - \int_0^T \int_\Omega \Big(\varepsilon\partial_t\varphi(\boldsymbol{x},t) - \varepsilon\Delta\varphi(\boldsymbol{x},t) + \frac{1}{\varepsilon}G'(\varphi(\boldsymbol{x},t)) + c_w\eta(\boldsymbol{x},t) + \lambda(t)\Big) p(\boldsymbol{x},t)\,d\Omega\,dt.$$

Requiring stationarity of the Lagrangian with respect to the adjoint state yields the state (forward) equation and requiring stationarity of the Lagrangian, at the optimal control η^* and associated optimal state φ^*, with respect to the state and the control, yields the (formal) first order optimality conditions

$$\delta_\varphi\mathcal{L}(\varphi^*,\eta^*,p)\varphi = 0, \forall\varphi : \varphi(\boldsymbol{x},0) = 0,$$
$$\delta_\eta\mathcal{L}(\varphi^*,\eta^*,p)\eta = 0, \forall\eta.$$

Optimality conditions [Tröltzsch, 2010]

Seeking optimality conditions yield the adjoint equation, which is the following linear parabolic PDE (posed backwards in time) for the adjoint state p,

$$\begin{cases} \partial_t p(\boldsymbol{x}, t) & = -\Delta p(\boldsymbol{x}, t) + \frac{1}{\varepsilon^2} G''(\varphi(\boldsymbol{x}, t)) p(\boldsymbol{x}, t) \quad \text{in } \Omega \times (T, 0], \\ \nabla p \cdot \boldsymbol{\nu} & = 0 \quad \text{on } \partial\Omega \times (T, 0], \\ p(\boldsymbol{x}, T) & = \varphi(\boldsymbol{x}, T) - \varphi_{obs}(\boldsymbol{x}) \quad \text{in } \Omega, \end{cases}$$

and together with the Riesz representation theorem yields the optimality condition for the control [Tröltzsch, 2010]

$$\delta_\eta \mathcal{L}(\varphi^*, \eta^*, p) = \theta \eta^* + \frac{1}{\epsilon} p = 0.$$

HPC Scientific Computing

- Cell-centred 2^{nd} order finite difference method (FDM) on rectangular grids
- PARAMESH library for mesh generation and parallelism
- Dynamic load-balancing for adaptive mesh refinement (AMR)
- Fully implicit 2^{nd} order backward differentiation formula (BDF2)
- Geometric nonlinear multigrid solution method using full approximation scheme (FAS) and multi-level adaptive technique (MLAT)
- Point-wise Newton linearisation with Gauss-Seidel iteration
- Full weighting restriction and multi-linear interpolation

Numerical challenges

- Each η iteration covers all time steps (both forward and backward)
- Memory requirement (let's consider double precision and 100 time steps)
  - 2-D: 512^2 requires 0.4 gigabytes
  - 3-D: 512^3 requires 215 gigabytes

Adaptive iterative update for the optimal control

- We denote a superscript ℓ for the η iteration, and at $\ell = 0$, we take

$$\eta^{\ell=0} = 0 \text{ on } \Omega \times [0, T)$$

  as our initial guess for the control.
- A gradient-based iterative update of the control, following the steepest descent approach, and the update is given by

$$\eta^{\ell+1} = \eta^{\ell} - \alpha \left(\theta \eta^{\ell} + \frac{1}{\epsilon} p^{\ell} \right), \text{ on } \Omega \times [0, T),$$

  where $\ell + 1$ denotes the next η iteration and ℓ indicates the current η iteration.
- The whole procedure is repeated until the objective function J satisfies some pre-defined tolerances.

Adaptive α

Algorithm

1. **While** the difference between consecutive Js is still large or J has not reached below a pre-defined tolerance **do**
2. Solve the forward Allen-Cahn equation in $\Omega \times (0, T]$
3. Compute the objective functional J^ℓ
4. **if** $J^\ell > J^{\ell-1}$ **and** $\ell > 0$ **then**
   $\alpha = max(\alpha \times \mathcal{P}_l, \alpha_{min})$
   restart = **TRUE**
   else if $J^\ell < J^{\ell-1}$ **and** $\ell > 0$ **then**
   $\alpha = \alpha \times \mathcal{P}_u$
   restart = **FALSE**
   end if
5. **if** restart == **FALSE then**
   Solve the backward adjoint equation in $\Omega \times [T, 0)$
   Backup the current η
   Compute the next η using α
   Continue to the next η iteration
   else
   Compute a new η using the latest backup with α
   Restart the current η iteration
   end if
6. **End**

Space and time discretisations of the forward and adjoint equations

- Spatial discretisation – Finite differences (2D and 3D)
- Time-stepping:
  1. BDF1 (also known as backward Euler method) is employed for the very first time step.
  2. BDF2 is employed for the remaining time steps
- $$\epsilon \frac{\varphi_{i,j,k}^{n+1,\ell+1} - \frac{4}{3}\varphi_{i,j,k}^{n,\ell+1} + \frac{1}{3}\varphi_{i,j,k}^{n-1,\ell+1}}{\tau} =$$
  $$\frac{2\epsilon}{3} D\left(\varphi_{i,j,k}^{n+1,\ell+1}\right) - \frac{2\left(-\varphi_{i,j,k}^{n+1,\ell+1} + \left(\varphi_{i,j,k}^{n+1,\ell+1}\right)^3\right)}{3\epsilon} + \frac{2\eta_{i,j,k}^{n+1,\ell+1}}{3} + \frac{2\lambda^{n+1}}{3},$$
- $\ell + 1$ denotes the current η iteration, $n+1$, n and $n-1$ indicate solutions from current, previous and the one before the previous time steps, respectively.
- We denote the 3-D Laplacian operator D as

$$D\left(\varphi_{i,j,k}\right) = \frac{\varphi_{i+1,j,k} + \varphi_{i-1,j,k} + \varphi_{i,j+1,k} + \varphi_{i,j-1,k} + \varphi_{i,j,k+1} + \varphi_{i,j,k-1} - 6\varphi_{i,j,k}}{h^2}.$$

Space and time discretisations of the forward and adjoint equations

- Within each time step, while solving for the solution of the above systems, we are also required to satisfy a given mass constraint.
- Iteratively determine the time-dependent, spatially-uniform volume constraint λ for the imposed mass constraint
- The Allen-Cahn system has to be solved multiple times, until a stopping criterion for λ is met.
- We denote this λ iteration using a superscript Λ, and its update follows the multi-step approach which is given as

$$\lambda^{n+1,\Lambda+1} = \lambda^{n+1,\Lambda} + \frac{\left(\lambda^{n+1,\Lambda} - \lambda^{n+1,\Lambda-1}\right)\left[M_{\varphi}^{n+1} - \int_{\Omega} \varphi^{n+1,\Lambda}\right]}{\left(\int_{\Omega} \varphi^{n+1,\Lambda} - \int_{\Omega} \varphi^{n+1,\Lambda-1}\right)}, \quad \text{for } \Lambda > 1,$$

  where M_{φ} is defined earlier, $\Lambda + 1$, Λ and $\Lambda - 1$ indicate values of λ from current, previous and the one before the previous λ iterations, respectively.
- Initial guesses

$$\lambda^{\Lambda=0} = -\frac{2\epsilon}{\tau} + 1, \quad \lambda^{\Lambda=1} = \frac{2\epsilon}{\tau} - 1.$$

- The stopping criterion used here is based upon the difference between consecutive values of λ.
- Providing a tolerance tol_{λ}, we consider the algorithm to have converged when $|\lambda^{n+1,\Lambda+1} - \lambda^{n+1,\Lambda}| < tol_{\lambda}$.

Approximation of the Optimal Control Problem

We propose a simple steepest-descent based iterative algorithm for the solution of the OC problem.

Algorithm

While tolerance not met:

1. Compute solution φ^n corresponding to control η^n. Mass constraint computed following [Blowey and Elliott, 1993].
2. Compute objective functional $J\left(\varphi^n, \eta^n\right)$ check if tolerance met.
3. Compute adjoint state p^n (for efficient computation of the gradient of J) requires the φ^n.
4. Update control according to gradient (i.e., compute η^{n+1}).
5. $n + 1 \to n$.

Efficiency

1. Adaptive parallel multigrid based solution method for the forward and adjoint problems.
2. "Two-grid" strategy: adaptive grid for forward problem, coarse uniform grid for (linear) adjoint problem. $\rightsquigarrow$ Massive memory savings.
3. Adaptive step-size selection for control update.

Multigrid: Two grid solution strategy

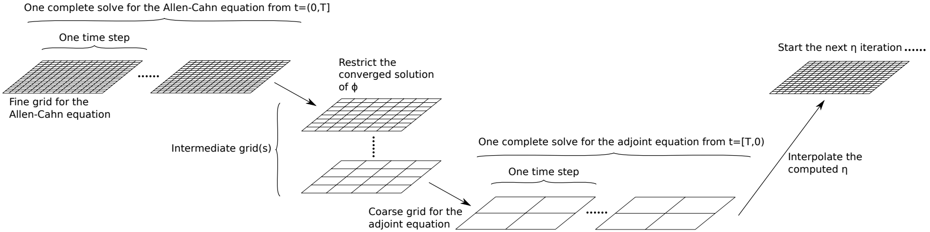

Two-grid scheme within multigrid V-cycles

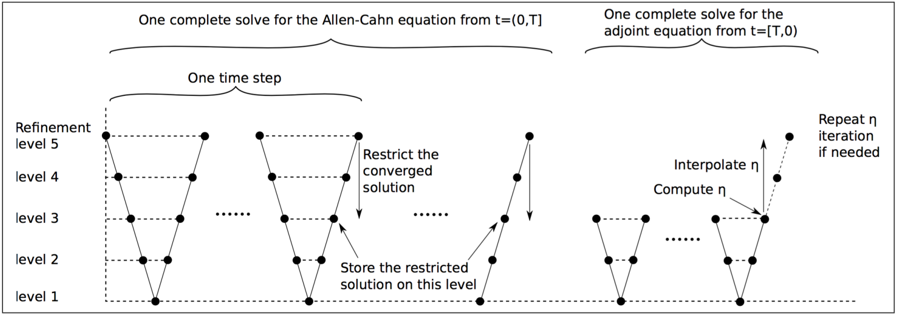

Circle to ellipse

A circle becomes two ellipses.

Desired data

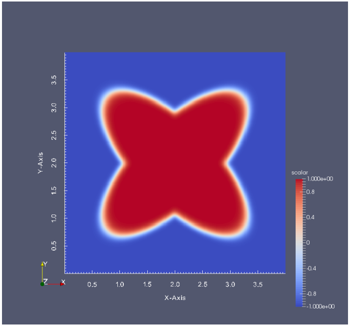

Initial data

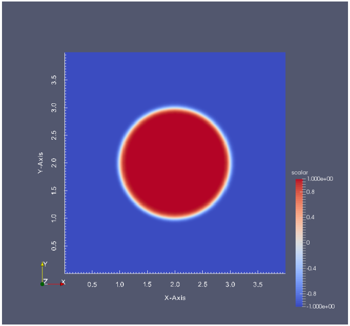

Geometric evolution of a circle to an ellipse

Convergence

$L_2(\Omega)$ error for φ			
	$m = t_1$	$m = t_2$	$m = t_3$
$d^m_{64^2}$	3.4264×10^{-2}	4.9226×10^{-2}	6.8561×10^{-2}
$d^m_{128^2}$	1.9721×10^{-2}	4.8058×10^{-2}	6.0397×10^{-2}
$d^m_{256^2}$	8.1793×10^{-3}	2.2300×10^{-2}	3.4557×10^{-2}
$d^m_{512^2}$	2.7850×10^{-3}	8.0407×10^{-3}	1.3192×10^{-2}
$L_2(\Omega)$ error for adjoint p			
	$m = t_1$	$m = t_2$	$m = t_3$
$d^m_{64^2}$	1.6773×10^{-2}	1.8048×10^{-2}	4.9344×10^{-2}
$d^m_{128^2}$	9.9721×10^{-3}	1.0158×10^{-2}	3.1554×10^{-2}
$d^m_{256^2}$	7.9290×10^{-3}	8.5311×10^{-3}	2.2551×10^{-2}
$d^m_{512^2}$	6.5082×10^{-3}	7.5551×10^{-3}	1.4901×10^{-2}
$L_2(\Omega)$ error for η			
	$m = t_1$	$m = t_2$	$m = t_3$
$d^m_{64^2}$	1.6976×10^{-1}	2.0752×10^{-1}	7.5240×10^{-1}
$d^m_{128^2}$	1.1923×10^{-1}	1.5793×10^{-1}	6.2554×10^{-1}
$d^m_{256^2}$	8.5093×10^{-2}	1.0601×10^{-1}	5.3023×10^{-1}
$d^m_{512^2}$	3.2344×10^{-2}	3.9359×10^{-2}	2.6302×10^{-1}

The convergence tests for the solutions of φ, adjoint p and η.

Multigrid convergence rates

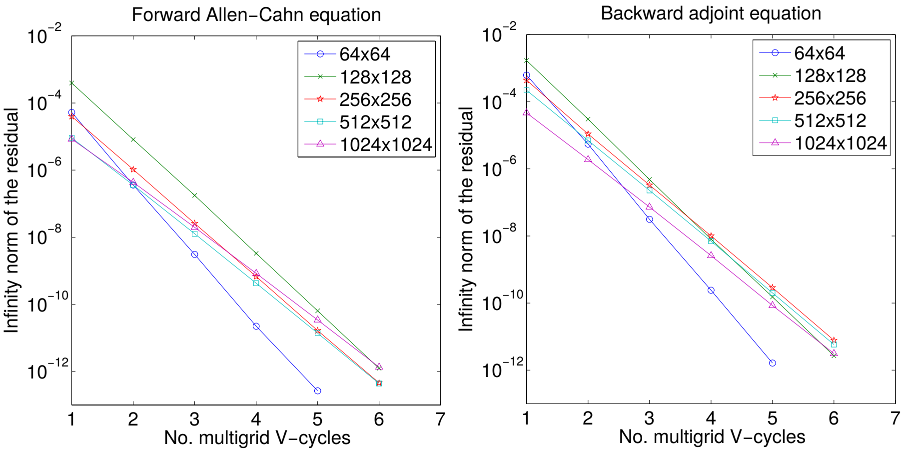

The multigrid convergence rates for the forward Allen-Cahn and backward adjoint equations.

Linear complexity of the multigrid method

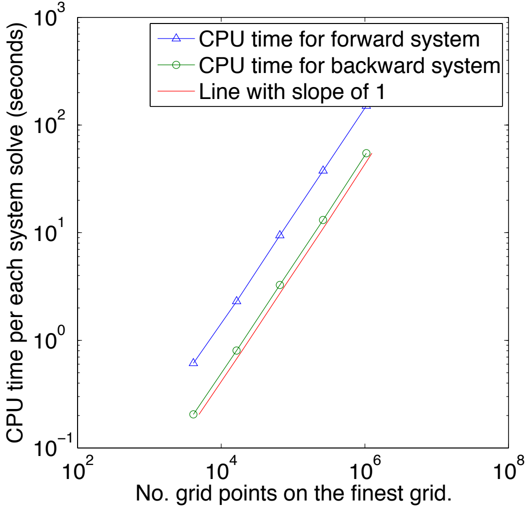

A log-log plot to illustrate the linear complexity of our multigrid solver. For comparisons, a line of slop 1 is included.

Dynamic Adaptive Mesh Refinement

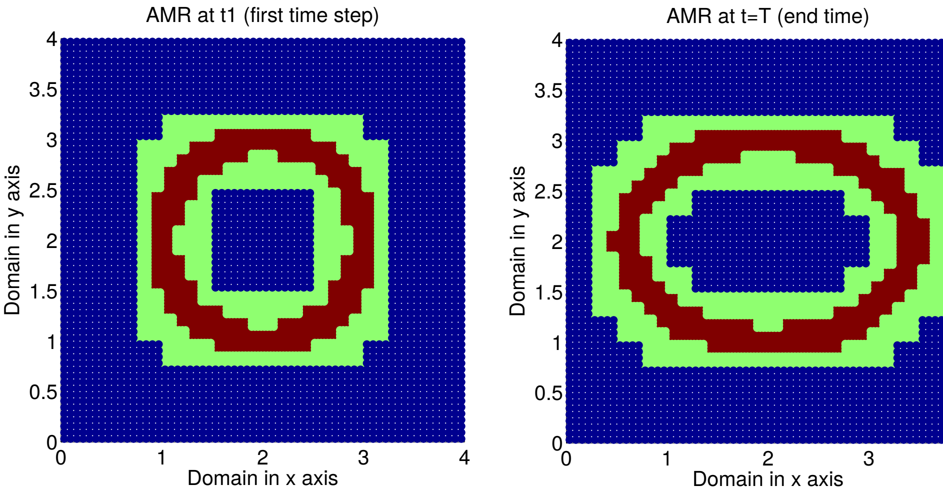

Two colour plots show the dynamic AMR in our solver. The blue region shows the 64^4 grid; light green region indicates the 128^2 grid; and finally red region illustrates the finest 256^2 grid. The colour version of this figure is online.

Convergence: Two-grid strategy

$L_2(\Omega)$ error for φ			
	$m = t_1$	$m = t_2$	$m = t_3$
$d^m_{128^2}$	1.2327×10^{-2}	2.6664×10^{-2}	3.8450×10^{-2}
$d^m_{256^2-64^2}$	8.6270×10^{-3}	1.6895×10^{-2}	3.2925×10^{-2}
$L_2(\Omega)$ error for adjoint p			
	$m = t_1$	$m = t_2$	$m = t_3$
$d^m_{128^2}$	9.2021×10^{-3}	9.7122×10^{-3}	3.0233×10^{-2}
$d^m_{256^2-64^2}$	1.0004×10^{-2}	1.4886×10^{-2}	2.7392×10^{-2}
$L_2(\Omega)$ error for η			
	$m = t_1$	$m = t_2$	$m = t_3$
$d^m_{128^2}$	9.7196×10^{-2}	1.2153×10^{-1}	5.3632×10^{-1}
$d^m_{256^2-64^2}$	7.7932×10^{-2}	1.4930×10^{-2}	5.9167×10^{-1}

Comparisons of errors between an adaptive two-grid simulation ($256^2 - 64^2$) with adaptive mesh refinement and a standard 128^2 uniform grid simulation.

Single cell imaging data

Initial and target Neutrophil shapes

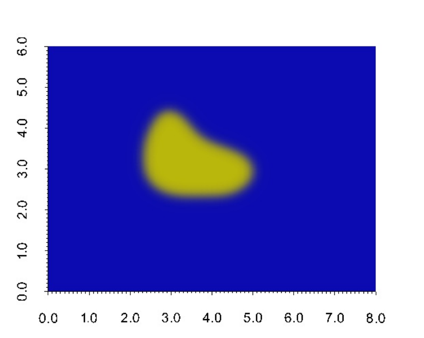

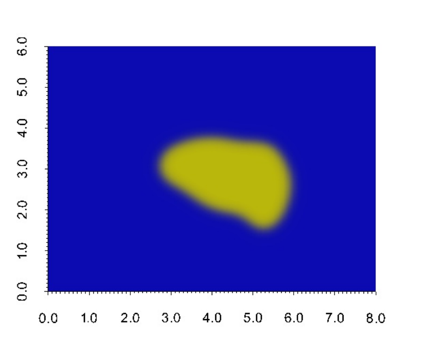

Single cell imaging data

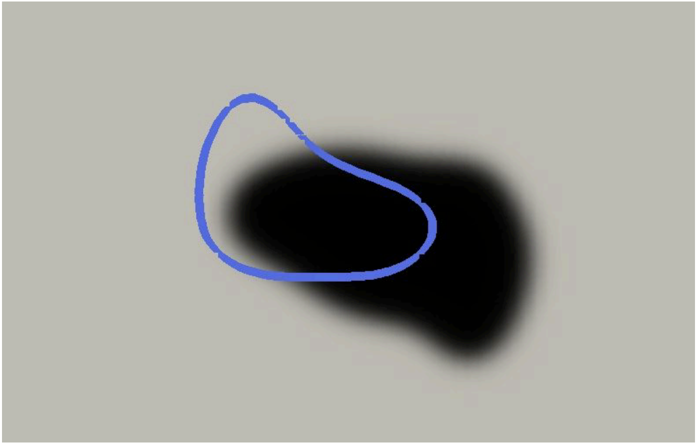

Zero level set of the computed surface shaded by the value of η and phase field representation of the target surface.

Cell one video

Cancer cell migration

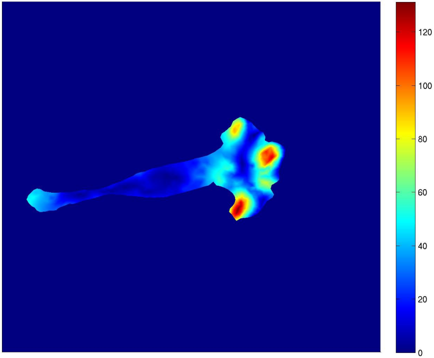

Data from [Peschetola, Laurent, Duperray, Michel, Ambrosi, Preziosi, and Verdier, 2013].

Keratocyte migration

Tracking topological changes during cell migration

For a smooth, oriented, compact (i.e., no boundary) surface Γ, the Euler number of a Riemann manifold (a topological invariant) is given by [Allendoerfer, 1940]

$$\chi = \frac{1}{2\pi}\int_\Gamma K \mathrm{d}\sigma$$

where K is the Gauss curvature of the surface.

2D case [Du, Liu, and Wang, 2005]

For $-1 < b < 0 < a < 1$

$$\chi_\varepsilon = \frac{1}{2\pi(a-b)}\int_{\Omega(a,b)}\left(-\Delta\varphi + \frac{\nabla|\nabla\varphi|^2\cdot\nabla\varphi}{2|\nabla\varphi|^2}\right)\mathrm{d}\vec{x} \approx \text{ \# of cells}$$

Future Work

Penalise changes in topology [Dondl, Mugnai, and Röger, 2011, 2014].

Application to quantifying cell proliferation rates: The MDCK cell line

Funding Acknowledgement

1. The Leverhulme Trust Research Project Grant (RPG-2014-149): *Unravelling new mathematics for 3D cell migration*, 2014 - 2017. £**259, 000**.
2. Royal Society Wolfson Research Merit Award Holder generously funded by the Royal Society and the Wolfson Foundation, 2016-2021. £**50, 000**.
3. Engineering and Physical Sciences Research Council Research Grant (EP/J016780/1): *Modelling, analysis and simulation of spatial patterning on evolving surfaces*, 2012-2015. £**401, 207**.
4. EU Horizon2020 MSCA-ITN-2014: *Integrated component cycling in epithelial cell motility*, 2015-2019. (11 Universities, 4 Research Institutes, and 4 Industrial Companies). **3.8*million*** Euros
5. South Africa Higher Education and Training and the British Council. University Capacity Development Programme (UCDP) Collaborative Project Proposal for Phase 2 of the University Staff Doctoral Programme (USDP): Building Caparcity in Applied Mathematics (USDP-BCAM). April 2020 - March 2024. SA Rand 6.25 million: **£165,000**.
6. Engineering and Physical Sciences Research Council (EPSRC - EP/T00410X/1). UK-Africa Postgraduate Advanced Study Institute in Mathematical Sciences (UK-APASI). April 2020 - March 2021, **£157, 000**.
7. The British Council. SA-UK USDP Phase 1: Initial Planning for Doctoral Training Centre. April - July 2019. **£10,000**.